A DISPLACEMENT ESTIMATOR FOR MAGNETIC BEARINGS

Elkin F. Rodriguez Velandia
UFF, PGMEC, r. Passo da Pátria 156, Niterói/RJ, 24210-240, Brasil
Elkinrodvel@msn.com

José Andrés Santisteban
UFF, PGMEC, TEE, r. Passo da Pátria 156, Niterói/RJ, 24210-240, Brasil
jasantisteban@vm.uff.br

Bruno Campos Pedroza
UFF, PGMEC, TDT, r. Passo da Pátria 156, Niterói/RJ, 24210-240, Brasil
bpedroza@uol.com.br

Abstract. *The research on magnetic bearings is being developed worldwide with relatively good success, Brazil included. Due to its multidisciplinary nature, a wide variety of conceptions have been proposed, in such a way that, while some authors look into dimensions and materials optimization, others propose improvements on the control technique. More recent are the approaches directed to eliminate the displacement sensors, in order to reduce costs and space. This work describes the practical implementation of a displacement estimator for a radial magnetic bearing. The results are compared with the displacement sensor signals from a prototype with magnetic bearings.*

Keywords*: Magnetic Bearings, Displacement Estimator, Industry Applications*

1. Introduction

The advantages of Active Magnetic Bearings (AMB) in many industrial applications are well known. Some of them are reported since the 70´s. As these devices allow operation without lubrication, elimination of vibrations and also high speeds, they are attractive to industry mainly in terms of costs, product quality, safety and environment protection (Schweitzer et al, 1994, Cheol-Soon et al, 1996, Gahler C. et al, 1996, An-Chen et al, 1996).

The classic design of AMB controllers supposes the existence of good displacement sensors. In the market may be found several types which depend on their operation principle. They can be capacitives, inductives, optics, eddy current type, Hall Effect, laser and so on. Nevertheless, the costs involved with the displacement sensors and with their mounting continue being high.

As a consequence, several alternatives to displacement sensors have been proposed, like the use of auxiliary windings mounted on the poles of AMB´s but also the use of observers. According to the literature may be found two types: complete-order and reduced-order, nevertheless, according to Takeshi et al (1995) complete-order observers are more robust than reduced-observers. Anyway, the drawbacks with observers are not few. By instance, the harmonics content generated by electronic drivers of AMB´s are superposed to the voltage and current signals so its influence must be taken into account when observers are designed. Additionally, if an economic approach is desired, the use of high speed processors to implement these observers may be a constraint. With this in mind, and having constructed a prototype of electric induction motor with AMB´s controlled with a microcomputer, in this work, a particular complete-order observer to measure displacement is evaluated.

2. Modelling

The prototype of electric induction motor with AMB´s has two radial units. In Fig. 1, left, one radial bearing stator is shown. Their eight coils can generate four resultant magnetic forces that operate in a differential manner, at the horizontal and vertical direction, e.g., to attract the rotor upwards, the resultant force created by the upper coil pair is increased, while the one created by the lower pair is decreased.

The stators of the axial magnetic bearings are composed of one coil each, producing a magnetic flux path that is closed by the axial airgaps and the axial bearing part of the magnetic bearing rotor. Hence, only one resultant Maxwell force is produced per bearing, which are opposed, one bearing to the other, and also operate in a differential way. Relative to the geometrical axis of the motor, these magnetic flux paths are axis symmetric.

The magnetic fields produced by the radial and axial magnetic bearing stators act upon the same component, the magnetic bearing rotor. As implicitly explained above, there is one axial magnetic bearing rotor placed at each side of the equipment shaft. The plane surfaces, external to the two bearing rotors, receive the axial action, while the cylindrical surfaces receive the radial action. In Fig. 1, right, the whole rotor shaft supporting the motor rotor and the magnetic bearing rotors are shown. In the same figure, upper, can be seen the two covers that in a compact way hold the stators of magnetic bearings. These covers also hold four inductive displacement sensors, axially displaced from the bearing stators, but located on the symmetry planes of the four radial magnetic pole pairs. In order to enhance their response,

each pair of radially opposing transducers also works in a differential way. Axial displacements, however, are measured by only one sensor. At the center, the rotation transducer cap is shown.

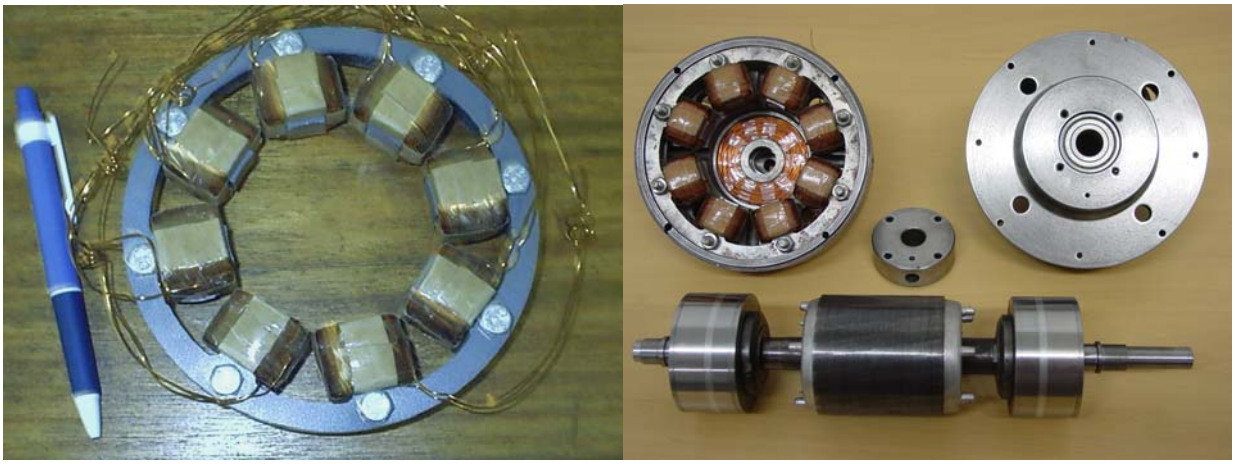

Figure 1. Magnetic bearing details. Left: one stator of radial AMB. Right: shaft with AMB rotors and caps.

2.1. Basic Relationships

In order to facilitate the design, suppose for a while that a radial magnetic bearing is supporting a disc with a concentrated mass *m* (Fig. 2) and considering the magnetic forces F_1 and F_2 acting along the horizontal axis "*x*" one has:

$$m\ddot{x} = F_1 - F_2 . \tag{1}$$

Where the magnetic forces F_k are determined as:

$$F_k = \frac{\Phi_k^2}{\mu_o A}, \tag{2}$$

where Φ_k is the net magnetic flux established by one coil pair, μ_0 is the vacuum magnetic permeability and *A* is the normal area to the airgap flux. The other relationships are (Mizuno et al, 1995):

$$NI_k = R_{mk}\Phi_k , \tag{3}$$

$$E_k = RI_k + N\dot{\Phi}_k . \tag{4}$$

Where E_k is the voltage imposed on the total winding, formed by one pair of coils, *R* its resistance, I_k the current, *N* the total number of coils and R_{mk} the total magnetic reluctance. Now, considering that the magnetic permeability on the airgap, D_k, is higher than the air magnetic permeability then:

$$R_{mk} = \frac{2D_k}{\mu_0 A} . \tag{5}$$

Combining Eqs. (1), (2), (3) and (5) one has:

$$m\ddot{x} = \frac{\mu_0 \mathrm{A} N^2 I_1^2}{4(D_0 - x)^2} - \frac{\mu_0 \mathrm{A} N^2 I_2^2}{4(D_0 + x)^2} = \frac{\mu_0 \mathrm{A} N^2}{4}\left[\frac{I_1^2}{(D_0 - x)^2} - \frac{I_2^2}{(D_0 + x)^2}\right], \tag{6}$$

where D_o is the equilibrium airgap. Actually, Eq. (6) must be multiplied by cos(α) as there is an angle (α = π /8) between the actual magnetic forces and the surface of the magnetic bearing rotors, leading to a net force F_{net} (Fig. 3).

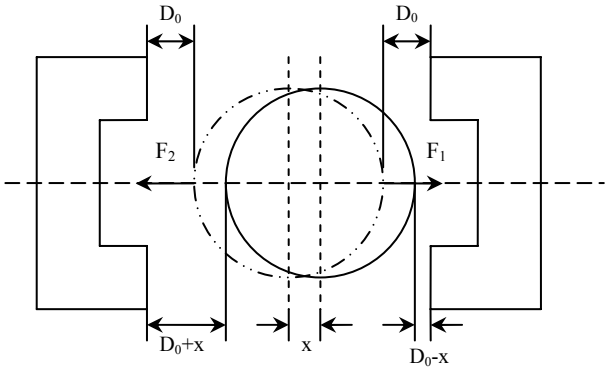

Figure 2. Magnetic forces acting along the horizontal axis.

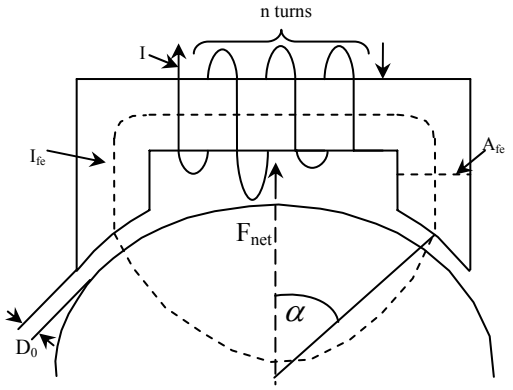

Figure 3. Actual geometry of a magnetic radial bearing.

2.2. Linearization and state space modelling

Defining individual currents I_k as a function of I_o, the bias current, and control currents i_1 and i_2 one has:

$$I_1 = I_o + i_1$$
$$I_2 = I_o + i_2 \tag{7}$$

Next, substituting Eq. (7) in Eq. (6) and considering that $x << D_0$ it is possible to obtain a linear relationship around the operation point: $x = 0$ and i_1 and i_2 equal to zero. Thus $f_x = F_1 - F_2$ is given by:

$$f_x = m\ddot{x} = k_i i + k_s x\ , \tag{8}$$

where:

$$i = i_1 - i_2 \tag{9}$$

$$k_i = \frac{(2kI_0)}{(D_0^{\,2})}\cos(\alpha), \tag{10}$$

$$k_s = \frac{(4kI_0^{\,2})}{(D_0^{3})}\cos(\alpha), \text{ and} \tag{11}$$

$$k = \frac{\mu_0 A N^2}{4}\ . \tag{12}$$

In this way:

$$\ddot{x} = \frac{k_i}{m} i + \frac{k_s}{m} x\ . \tag{13}$$

As was mentioned at the beginning of 2.1, this relationship was conceived supposing a concentrated mass "*m*" in the center of a thin disc. However, in the actual situation, it must be considered that four radial mechanical degrees of freedom are being controlled. In this case the gravity center is not more in the same plane of the radial stator of AMB. With this in mind, Eq. (13) must be modified taking into account the classic modeling of a rigid rotor. Thus, considering the axial displacement without influence in the other ones and according to Schweitzer, 1994, the axis can be modeled as:

$$\mathbf{f}_B = \mathbf{M}_B \ddot{\mathbf{Z}}_B + \mathbf{G}_B \dot{\mathbf{Z}}_B\ , \tag{14}$$

where $\mathbf{f_B}$ is the column vector representing all the radial magnetic forces and column vector $\mathbf{Z_B}$ represent all the radial measured displacements. $\mathbf{M_B}$ and $\mathbf{G_B}$ are originated from linear algebraic transformations, where:

$\mathbf{M_B} = \mathbf{T_B^T}.\mathbf{M}.\mathbf{T_B}$, $\mathbf{G_B} = \mathbf{T_B^T}.\mathbf{G}.\mathbf{T_B}$ and:

$$\mathbf{M} = \begin{bmatrix} m & 0 & 0 & 0 \\ 0 & I_Y & 0 & 0 \\ 0 & 0 & m & 0 \\ 0 & 0 & 0 & I_x \end{bmatrix}, \qquad \mathbf{G} = \begin{bmatrix} 0 & 0 & 0 & 0 \\ 0 & 0 & 0 & 1 \\ 0 & 0 & 0 & 0 \\ 0 & -1 & 0 & 0 \end{bmatrix} I_z \Omega, \qquad \mathbf{T_B} = \frac{1}{b-a} \begin{bmatrix} b & -a & 0 & 0 \\ -1 & 1 & 0 & 0 \\ 0 & 0 & b & -a \\ 0 & 0 & -1 & 1 \end{bmatrix}.$$

Above, *m* is the net mass of the shaft, that include the rotor mass of the motor, the rotor of the AMB´s and its axis, *Ix*, *Iy* and *Iz* are the inertia moments in respect to the center of mass of the whole rotor and Ω is the motor rotational velocity. $\mathbf{T_B}$ is used to transform the center of mass coordinates into the magnetic bearings coordinates, one for each axis. Finally, '*a*' and '*b*' are the distances from the rotor center of mass to each radial magnetic bearing.

In order to design displacement controllers, Eq. (14) can be transformed as in Eq. (15) below, where $\mathbf{M_{Bi}}$ is the inverse of matrix $\mathbf{M_B}$ and $\mathbf{MG} = \mathbf{M_{Bi}} \times \mathbf{G_B}$.

$$\ddot{\mathbf{Z}}_\mathbf{B} = \mathbf{M_{Bi}} \times \mathbf{f_B} - \mathbf{MG} \times \dot{\mathbf{Z}}_\mathbf{B} \tag{15}$$

The matrix $\mathbf{M_{Bi}}$ and $\mathbf{MG}$ have the following forms:

$$\mathbf{M_{Bi}} = \begin{bmatrix} \frac{(m a^2 + I_y)}{m I_y} & \frac{(m a b + I_y)}{m I_y} & 0 & 0 \\ \frac{(m a b + I_y)}{m I_y} & \frac{(m b^2 + I_y)}{m I_y} & 0 & 0 \\ 0 & 0 & \frac{(m a^2 + I_x)}{m I_x} & \frac{(m a b + I_x)}{m I_x} \\ 0 & 0 & \frac{(m a b + I_x)}{m I_x} & \frac{(m b^2 + I_x)}{m I_x} \end{bmatrix}, \tag{16}$$

$$\mathbf{MG} = \begin{bmatrix} 0 & 0 & \frac{a I_z \Omega}{I_y (a-b)} & -\frac{a I_z \Omega}{I_y (a-b)} \\ 0 & 0 & \frac{b I_z \Omega}{I_y (a-b)} & -\frac{b I_z \Omega}{I_y (a-b)} \\ -\frac{a I_z \Omega}{I_x (a-b)} & \frac{a I_z \Omega}{I_x (a-b)} & 0 & 0 \\ -\frac{b I_z \Omega}{I_x (a-b)} & \frac{b I_z \Omega}{I_x (a-b)} & 0 & 0 \end{bmatrix}. \tag{17}$$

This leads to a block diagram with four inputs and four outputs. It is depicted below:

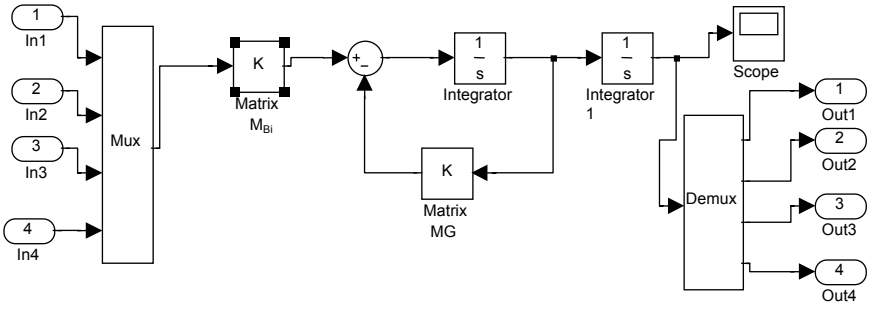

Figure 4. Mechanical model of the rotor.

At this point, considering that this is a first version of an estimator using an observer, the speed of the rotor was considered null, then the matrix **MG** in Eq.(17) is also null. In this way, combining Eq. (15) with Eq. (8), and considering that the orthogonal axis is in equilibrium, what means zero control current and zero displacement in the axis "y", Eq. (13) changes to:

$$\ddot{x} = \left(\frac{a^2 m + I_x}{I_x m} \right) k_i i + \left(\frac{a^2 m + I_x}{I_x m} \right) k_s x \,. \tag{18}$$

Now, taking Eq. (4), a linearization procedure, as done with Eq. (6) to obtain Eq. (8), can be applied. In this way:

$$E_k = E_o + e_k \,. \tag{19}$$

So for each opposite winding voltage e_k is given as:

$$e_1 = K_b \dot{x} + R i_1 + L \dot{i}_1 \,, \tag{20}$$

$$e_2 = -K_b \dot{x} + R i_2 + L \dot{i}_2 \,. \tag{21}$$

Where: $L = \dfrac{\left(N^2 \mu_0 A\right)}{\left(2D_0\right)}$ and $k_b = \dfrac{\left(\mu_0 A N^2 I_0\right)}{\left(2D_0^{\,2}\right)}$.

Next, defining $u = e_1 - e_2$, from (16) and (17) one has:

$$\dot{i} = -\frac{2K_b}{L}\dot{x} - \frac{R}{L} i + \frac{1}{L} u \,. \tag{22}$$

Then, with Eqs. (14) and (18) a state-space representation may be given as:

$$\begin{aligned} \dot{\mathbf{z}} &= \mathbf{A}\mathbf{z} + \mathbf{B}u \\ w &= \mathbf{C}\mathbf{z} \end{aligned} \,, \tag{23}$$

where:

$$\mathbf{z}(t) = \begin{bmatrix} x \\ \dot{x} \\ i \end{bmatrix}, \quad \mathbf{A} = \begin{bmatrix} 0 & 1 & 0 \\ \left(\dfrac{a^2 m + I_x}{I_x m} \right) k_s & 0 & \left(\dfrac{a^2 m + I_x}{I_x m} \right) k_i \\ 0 & \dfrac{-2k_b}{L} & \dfrac{-R}{L} \end{bmatrix},$$

$$\mathbf{B} = \begin{bmatrix} 0 \\ 0 \\ \dfrac{1}{L} \end{bmatrix} \text{ and } \mathbf{C} = \begin{bmatrix} 0 & 0 & 1 \end{bmatrix}.$$

3. Observer design

In control theory, as known, the usual design rule consists in develop a state feedback controller before to design a full-order observer. Nevertheless, as our main objective was to test only the performance of one observer, the state feedback controller was not implemented but only simulated. The actual control of the electric motor prototype with AMB was not modified. It consists on displacement controllers based in models that consider currents as inputs and displacements as outputs. In this way, as in Eq. (23) the winding voltage is considered as input and the current as output, the pole placement criterion was applied in such a way that the displacement response of the state feedback

controller be coincident with the actual prototype response. Thus, the desired poles were chosen taking into account this behavior and given as: (-56±57.13i) sec^{-1} and -3000 sec^{-1}. As a design tool, the Ackermann method was adopted (Ogata, 2003).

With m= 5.3042 kg, I_x=50.3e-6 kg-m^2, a=-68.9e-3 m, K_b=173.7163 N/A, R =2 Ω, L=0.0604 H, Ki=160.4930 N/A and Ks= 2.3075e+005 N/m in Eq. (23) and with $\det[s\mathbf{I}-\mathbf{A}+\mathbf{BK}]=0$ the state feedback matrix **K** was obtained. In Eq. (24) its numerical components are shown. Next, choosing the roots of $\det[s\mathbf{I}-\mathbf{A}+\mathbf{L}_e\mathbf{C}]=0$ as: (-112±114.26i) sec^{-1} and -5000 sec^{-1} the observer gain matrix $\mathbf{L}_e$ was determined. In Eq. (25) are shown its numerical components. In Fig. 5 the block diagram of the observer simulation is shown.

$$\boldsymbol{K}=\begin{bmatrix}2.7034e^{5} & -259.23 & 185.98\end{bmatrix}, \tag{24}$$

$$\boldsymbol{L}_e=\begin{bmatrix}-0.90925\\ 11184\\ 5190.9\end{bmatrix}. \tag{25}$$

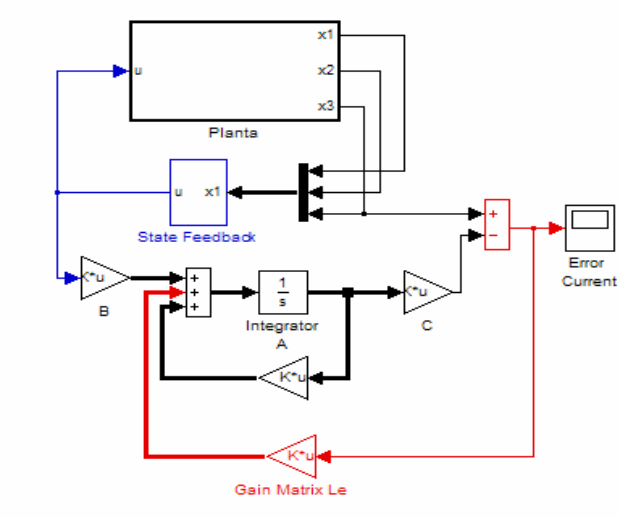

Figure 5. Block diagram used for observer simulation.

4. Experimental Results

In order to implement the observer, the winding currents were measured with effect–hall sensors. The voltages on two opposite coils was monitored through resistive divisors and subtracted before to go to the computer. Analogous procedure was made with the currents. Additionally, as both current and voltages were quite noising, two first-order filters were used. These were implemented with operational amplifiers, having unity gain and their domain poles was designed to be -833.33 sec^{-1}.

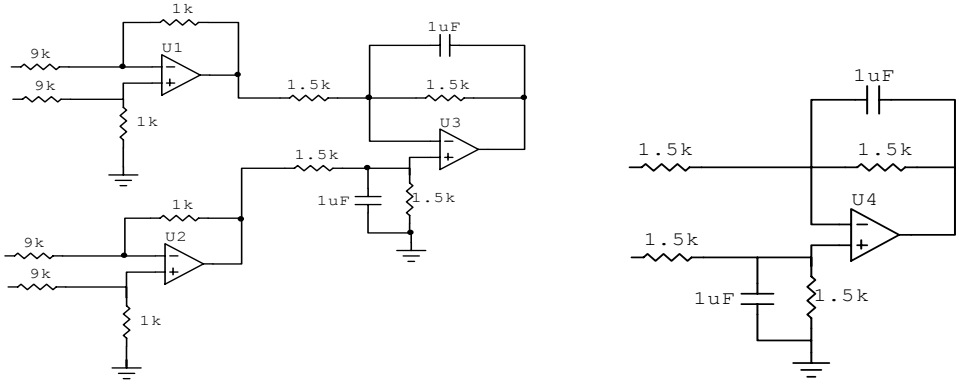

Figure 6. Analog circuits to measure winding voltages (left) and winding currents (right).

The discretization of the observer, with a sampling frequency of 1 kHz, lead to the following difference equations (Ogata, 1994):

$$z1_k = 3.4039e^{-6}u_k + 1.4222z1_{k-1} + 1.1832e^{-4}z2_{k-1} + 2.8686e^{-4}z3_{k-1} + 1.0513e^{-4}\left[i_{k-1} - z3_{k-1}\right],$$
$$z2_k = 4.7491e^{-3}u_k + 2581{,}8z1_{k-1} - 0.22777z2_{k-1} + 1.7863z3_{k-1} + 2.3867\left[i_k - z3_{k-1}\right],$$
$$z3_k = -2.9454e^{-3}u_k + 2372.3z1_{k-1} - 0.67695z2_{k-1} - 0.6441z3_{k-1} - 0.61791\left[i_k - z3_{k-1}\right],$$

where the subscript k is related to the sampling time.

In the equilibrium point, the static response of the observer was compared with the real position measured with an eddy-current displacement sensor as shown in Fig. 7.

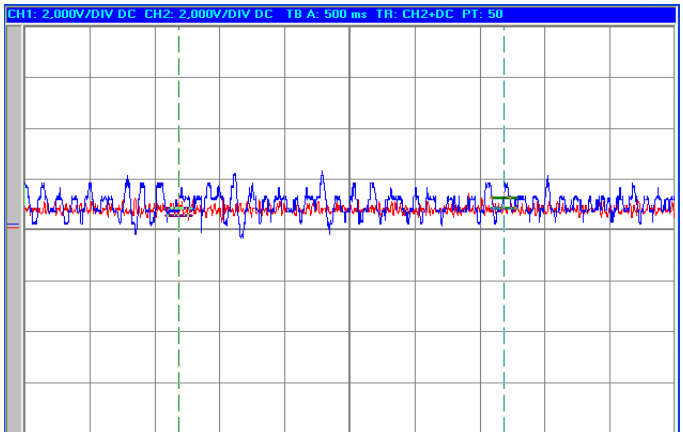

Figure 7. Signals from displacement sensor (red) and observer (blue).
Scale: 0.5 sec/div, Ver: 0.15mm/div

In Fig. 8 the dynamic response of the observer when the displacement reference changes from -0.3mm to 0.25mm in 7 seconds is shown.

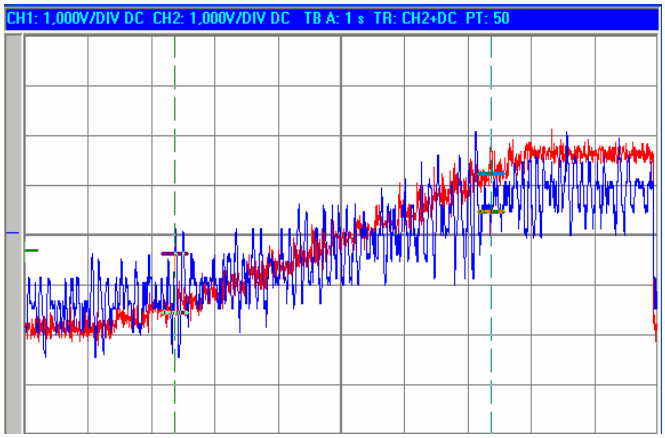

Figure 8. Signals from displacement sensor (red) and observer (blue).
Scale: Hor: 1sec/div, Ver: 0.07mm/div

Finally, in Fig. 9 the dynamic response of the observer when the displacement position is changing at 0.4 Hz from -0.15mm to 0.15mm is shown. The observer delay between signals is about 100ms. Many reasons may explain this fact but one of them is that in this version of observer was not considered the couplings shown by matrix $\mathbf{M}_{Bi}$.

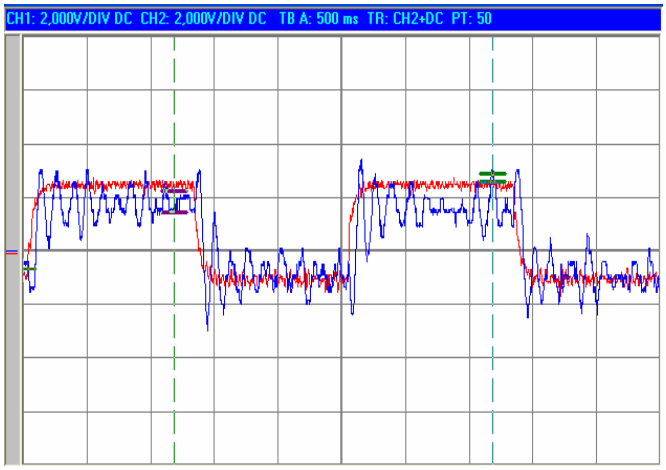

Figure 9. Signals from displacement sensor (red) and observer (blue). Scale: Hor: 0.5sec/div, Ver: 0.15mm/div.

5. Conclusions

This work briefly describes the design and implementation of one version of a displacement estimator based in a full-order observer to be used with active magnetic bearings.

Although experimental results show that this estimator is not yet fast to substitute the displacement sensor, for applications where slow changes in displacement are expected, these results may be considered satisfactory.

This implementation has shown the utility of auxiliary analog circuits to reduce the effort of the digital processors with limited speed, as it was in this case using a personal computer.

6. Acknowledgements

The authors gratefully acknowledge the support of CNPq and CAPES.

7. References

An-Chen Lee., Yi-Hua Fan, 1996, “Decentralized PID Control of Magnetic Bearings in a Rotor System”, Fifth International Symposium on magnetic Bearings Kanazawa, Japan, pp 13-16.

Cheol-Soon Kim, Chong-Won Lee, 1996, “In-situ Runout identification in Active Magnetic Bearing System by Extended Influence Coefficient Method”, Fifth International Symposium on magnetic Bearings Kanazawa, Japan, pp 1-6.

Gahler C., Mohler M., Herzog R., 1996, “Multivariable Identification of Active Magnetic Bearing Systems”, Fifth International Symposium on magnetic Bearings Kanazawa, Japan, pp 7-12.

Noronha, R.F., Lima, L.T.G., Leite Jr., T.M.,Gomes G.M.P. and Santos P.C.V., 2000, “Dynamic Behavior of a Magnetically Borne Rotor”, Proceedings of the 16th International Conference on Magnetically Levitated Systems and Linear Drive –MAGLEV 2000, Rio de Janeiro, pp. 456-461.

Ogata, K., 1970, “Engenharia de Controle Moderno”, 4a Ed, Prentice Hall do Brasil Ltda, 782 p.

Ogata, K., 1994, “Discrete-Time Control Systems”, Pearson Education.

Santisteban, J.A., Noronha, R,F., David, D.F.B., Suhett, M.R. and Pedrosa, J.F.A., 2004, “Implementation of Magnetic Bearings on an Electric Motor”, Proceedings of the VI Induscon, Joinville, SC, Brasil.

Schweitzer, G., Blueler, H. and Traxler, A., 1994, “Active Magnetic Bearings”, v/dlf Hochschulverlag AG an der ETH Zürich, Suíça.

Mizuno T., Araki K., Bleuler H., 1995, “On the Stability of Controllers for Self-Sensing Magnetic Bearings”, SICE 95 Proceeding of the 34th SICE Annual Conference International Session, Sapporo, Japan, pp 1599-1604.

5. Responsibility notice

The authors are the only responsible for the printed material included in this paper.